Chapter 4

Plate tectonics on the terrestrial planets

Abstract

Plate tectonics is largely controlled by the buoyancy distribution in oceanic lithosphere, which correlates well with the lithospheric age. Buoyancy also depends on compositional layering resulting from pressure release partial melting under mid-ocean ridges, and this process is sensitive to pressure and temperature conditions which vary strongly between the terrestrial planets and also during the secular cooling histories of the planets. In our modelling experiments we have applied a range of values for the gravitational acceleration (representing different terrestrial planets), potential temperatures (representing different times in the history of the planets), and surface temperatures in order to investigate under which conditions plate tectonics is a viable mechanism for the cooling of the terrestrial planets. In our models we include the effects of mantle temperature on the composition and density of melt products and the thickness of the lithosphere. Our results show that the onset time of negative buoyancy for oceanic lithosphere is reasonable (less than a few hundred million years) for potential temperatures below $\sim 1500^oC$ for the Earth and $\sim 1450^oC$ for Venus. In the reduced gravity field of Mars a much thicker stratification is produced and our model indicates that plate tectonics could only operate on reasonable time scales at a potential mantle temperature below about $1300 - 1400^oC$.

4.1 Introduction

Plate tectonics is characterized by mid-ocean ridges, where oceanic crust and underlying depleted mantle is created by partial melting of upwelling mantle material, and subduction zones, where oceanic lithosphere including the basaltic crust moves underneath another

This chapter has been submitted by P. van Thienen, N.J. Vlaar and A.P. van den Berg for publication in *Physics of the Earth and Planetary Interiors*.

oceanic or a continental lithosphere into the underlying mantle. The two main driving forces for the plate tectonic process are ridge push and slab pull, of which the latter is generally an order of magnitude larger than the former (Turcotte and Schubert, 2002). Slab pull is caused by negative buoyancy of the cold descending lithosphere which may include the effect of the uplift of the olivine-spinel phase boundary in the cold slab. Resistive forces originate from friction and, in case the slab reaches this depth, a downward deflection of the spinel-postspinel phase boundary around 670 km depth. In order to make plate tectonics work, the plates must have sufficient negative buoyancy. Furthermore, the plates must conform to specific mechanical properties. They must act as stress guides and be strong enough to withstand the high tensional stresses associated with slab pull, which are on the order of 1 GPa (Turcotte and Schubert, 2002), while being able to bend at the subduction zone (e.g. Conrad and Hager, 2001).

Geologists interpret rocks from Archean and Proterozoic cratons as evidence for the beginning of modern style plate tectonics sometime between 4.0 Ga (De Wit, 1998) and 2.0 Ga (Hamilton, 1998), with the difference between these ages mainly stemming from the interpretation of rocks as either an equivalent of modern arc setting material or something with significantly different characteristics. But whatever the timing, at some point in the Earth's thermal evolution the force balance and mechanical properties of an oceanic type lithosphere became favorable for plate tectonics.

A suitable diagnostic for the buoyancy and gravitational stability of the oceanic lithosphere is the density defect thickness $d.d.t.$ (Oxburgh and Parmentier, 1977):

$$d.d.t. = \int \left(\frac{\rho_m - \rho}{\rho_m} \right) dz \tag{4.1}$$

In this expression, ρ_m is the density of the underlying mantle, ρ the local temperature and composition dependent density, and z the depth coordinate. The integral is taken over the thickness of the lithosphere. This parameter indicates whether a column of oceanic lithosphere experiences a net buoyancy force in upward or downward direction. Whether a net force results in actual vertical movement also depends on resistive forces and the mechanical properties of the lithosphere (e.g. Conrad and Hager, 2001). We also note that the criteria for starting and maintaining plate tectonics are not necessarily the same (see McKenzie, 1977; Sleep, 2000; Stevenson, 2003). Since in a hotter Earth, a thicker low density crust and thicker subcrustal layer of light depleted melt residue would be produced from upwelling material, the resulting lithosphere is more buoyant and therefore more difficult to subduct (Sleep and Windley, 1982; Vlaar, 1985). Vlaar and Van den Berg (1991) present modelling results of the development of the density defect thickness for oceanic lithosphere produced in a hotter Earth, showing that it takes a significantly longer cooling period (on the order of hundreds of millions of years) for oceanic lithosphere to become negatively buoyant, whereas for present-day Earth-like conditions, gravitational instability sets in at an age of ~ 30 million years. However, we also see younger crust subducting, indicating that lithospheric buoyancy does not completely determine the dynamics.

Numerical mantle convection models of subduction zones (using a composite rheology model including diffusion creep, dislocation creep and a stress limiter) for higher than present-day mantle temperatures show that for potential temperatures of 1525^{o}C and higher, subduction is eventually stopped by the reduced (temperature dependent) strength of the lithosphere (Van Hunen, 2001; Van Hunen et al., 2003); this results in frequent break-off of the subducting slab, which, in turn, prevents the buildup of sufficient slab pull.

An important consequence of one of the main distinguishing features between the terrestrial planets, the gravitational acceleration, is that on smaller planets a much thicker stratification could be developed as a result of partial melting in hot upwelling mantle, because under reduced gravity and pressure conditions the solidus and liquidus pressures correspond to greater depths. This effect is demonstrated in the work of Schott et al. (2001) on mantle convection models including compositional differentiation by pressure release partial melting of the Martian mantle. Such a thicker stratification is more buoyant, and therefore we can already predict that plate tectonics will be more difficult on Mars than on Earth.

It is clear from space observation that both Mars and Venus do not have plate tectonics nowadays (e.g. Zuber, 2001; Nimmo and McKenzie, 1996). We do not know, however, if in the earlier history of these planets plate tectonics has been active (Turcotte et al., 1999; Sleep, 1994, 2000). Satellite measurements of crustal magnetization on the southern hemisphere of Mars show a pattern more or less similar to magnetic striping found on the Earth's ocean floor, though both the width and signal magnitude are much larger than on Earth (Acuña et al., 1999; Connerney et al., 1999). Venus is thought to have undergone a global resurfacing event between 300 and 600 Myr ago (Schaber et al., 1992; Nimmo and McKenzie, 1998). Therefore we do not observe earlier material from which information can be obtained. No evidence is found for plate tectonics after the resurfacing.

In this work we will investigate under which thermal conditions plate tectonics may take place on terrestrial planets on the basis of buoyancy considerations. The dependency of the density defect thickness and specifically the time required for an oceanic lithosphere to obtain neutral buoyancy will be determined as a function of gravitational acceleration, representative of different planets, and potential temperature, representing different times in the thermal evolution of the planets subject to secular cooling. We model the lithospheric column as it would be produced at a mid-ocean ridge using a melting model for peridotite. A range of lithosphere thicknesses, corresponding to estimates for the present and early Earth, Mars and Venus is used in combination with a 1D numerical conductive cooling model to determine the cooling history of the lithosphere, and from this, the density defect thickness time series.

4.2 Description of the numerical models

4.2.1 Equations and procedure

The modeling approach presented here is an extension of that of Vlaar and Van den Berg (1991), using a 1-D melting model of McKenzie (1984). The main differences between their work and the present approach are (1) our inclusion of the effect of melting temperature on the composition and density of oceanic crust and (2) our use of different lithosphere thicknesses representative of the different terrestrial planets. The effect of the first point is that the increased buoyancy expected for a thicker crust, that is produced in a hotter mantle, is balanced by its higher density. The second modification mainly causes a steeper geotherm and, therefore, higher temperatures in the lower crust compared to the case with a (greater) constant lithosphere thickness. The sensitivity of the model to lithosphere thickness will be investigated below. The model is based on a 1-D evaluation of an adiabatically rising column beneath a mid-ocean ridge. In the region between solidus and liquidus in p,T-space, the pressure derivative of the melt fraction by weight F can be derived (see Vlaar and Van den Berg, 1991):

$$\frac{dF}{dp} = \frac{-\frac{c_p}{T}\left(\frac{\partial T}{\partial p}\right)_F + \frac{\alpha}{\rho}}{\Delta S + \frac{c_p}{T}\left(\frac{\partial T}{\partial F}\right)_p} \tag{4.2}$$

For an explanation of the symbols, see Table 4.1. The ordinary differential equation (ODE) (4.2) is integrated numerically in p using a fourth order Runge-Kutta scheme, starting from a surface value of the degree of melting, corresponding to a given extrusion temperature (see Figure 4.1). For any integration step, the temperature, occurring in the right hand side of the ODE (4.2) is computed from the parameterization of the phase diagram for mantle peridotite. The parameterization is based on polynomial approximations of the liquidus $T_L(P)$ and solidus $T_S(P)$, based on data from Herzberg and Zhang (1996), and the isobaric variation between 0 and 1 of F between liquidus and solidus, based on McKenzie and Bickle (1988). Integration of equation (4.2) is stopped when the solidus is reached, marking the deepest melting in the column. The corresponding temperature profile is calculated simultaneously from the solidus, liquidus and melting curve parameterizations for local pressure and corresponding F values.

The inclusion of the overburden pressure of the crust thus produced refines the solution in a number of iterative steps, and reduces the amount of basaltic crust produced (see Vlaar and Van den Berg, 1991). In order to do this, we need to account for the density of the basaltic crust. As we are considering the complete crust, we account for the average composition and corresponding average density, disregarding any differentiation processes in the crust that result in denser cumulates at the bottom and shallow lighter residual phases. We parameterize the crustal density as a function of T_{ex} (the temperature at which magma erupts at the surface). A relation between T_{ex} and MgO content of primitive magmatic rocks has been described by Nisbet (1982). The MgO content affects the mineralogy of these rocks and, thus, also the density. Generally, primitive rocks

symbol	property	value/unit
c	basalt solidification contraction	0.90
c_p	specific heat mantle	1250 $\mathrm{Jkg^{-1}K^{-1}}$
c_p	specific heat crust	1000 $\mathrm{Jkg^{-1}K^{-1}}$
F	mass fraction of melt	-
p	pressure	Pa
T	temperature	$^{\mathrm{o}}\mathrm{C}$
α	thermal expansion coefficient	$3 \cdot 10^{-5}\mathrm{K^{-1}}$
$\delta\rho$	density decrease upon full depletion	-226 $\mathrm{kgm^{-3}}$
ΔS	entropy change upon full melting	300 $\mathrm{Jkg^{-1}K^{-1}}$
κ	thermal diffusivity	$10^{-6}\mathrm{m^2s^{-1}}$
ρ	mantle density	3416 $\mathrm{kgm^{-3}}$
ϕ	residual melt fraction	0.01

Table 4.1: Relevant parameters used in the melting and cooling models.

with higher MgO contents have a higher density. For 58 published analyses of basalts, komatiitic basalts and komatiites, and a picrite (see Figure 4.2) we computed the CIPW normative composition in terms of mineral phases (e.g. Philpotts, 1990), and we calculated bulk rock densities using individual mineral densities (including the effect of iron content on the densities of olivine and the pyroxenes). A least squares best fit of the resulting densities as a function of T_{ex} (i.e., MgO content) was constructed:

$$\rho = 1500 + 1.925 \cdot T_{ex} - 5.153 \cdot 10^{-4} T_{ex}^2 \tag{4.3}$$

where ρ is the density of the solidified melt product (kgm^{-3}). The parameterized density (4.3) is shown as the dashed curve in Figure 4.2. Although the mantle composition of Venus and Mars may be slightly different from the Earth's mantle, we assume expression (4.3) to be valid for these planets as well.

Resulting crustal thicknesses for Earth and Mars are shown in Figure 4.3, together with earlier results from McKenzie and Bickle (1988), and based on those by Sleep (1994), and by Vlaar and Van den Berg (1991). Vlaar and Van den Berg (1991) show that it is important to include the effect of crustal overburden. This results in significantly smaller crustal thicknesses than those found by McKenzie and Bickle (1988) and Sleep (1994). Our results are consistent with those of Vlaar and Van den Berg (1991), the slightly smaller thicknesses in our Earth case resulting from the inclusion of the effect on melt product density of the potential temperature and the use of different parameterizations of solidus, liquidus and melting curve.

Using a specified surface temperature and the potential temperature extrapolated to the depth of the base of the lithosphere as boundary conditions, the evolution of the temperature profile is computed for the lithosphere by solving the time dependent 1-D heat equation for the cooling of a column of oceanic lithosphere with a second order finite difference scheme and Crank-Nicolson time integration. For each experiment, a constant

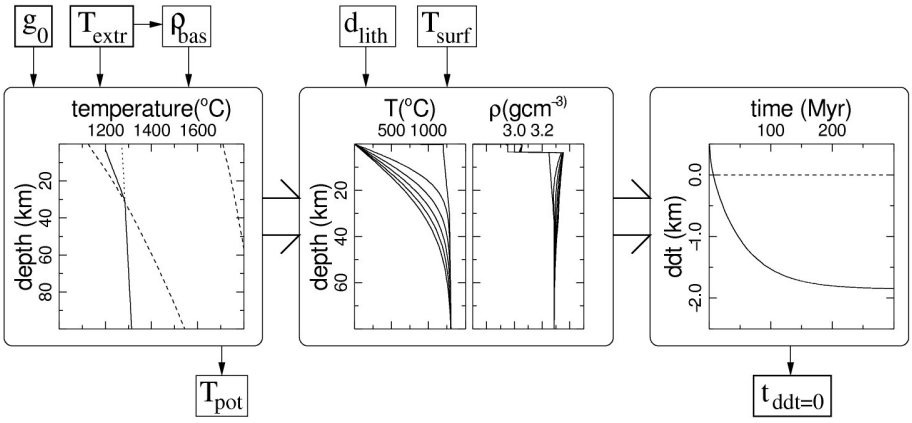

Figure 4.1: Experimental setup. From a prescribed magma extrusion temperature (which also gives the crustal density through equation (4.3)) and gravitational acceleration, a geotherm, material stratification (crust+depleted root) and corresponding density profile are calculated. Using a prescribed lithosphere thickness as the domain extent for finite difference calculations and using a prescribed surface temperature as the top boundary condition, the development of the geotherm is integrated in time and corresponding density profiles are again computed. The development of the density defect thickness, calculated using expression (4.1), is thus evaluated as a function of time and the zero buoyancy age is found.

domain size is used, spanning the depth of the lithosphere in thermal equilibrium (far from the ridge).

The use of a finite plate thickness in the same spirit as the analytical plate models of McKenzie (1967), Crough (1975), Doin and Fleitout (1996), and Dumoulin et al. (2001) allows for a balance to set in between the bottom heat flux into the lithosphere and the top boundary heat flux; this results in a steady state situation, whereas a halfspace model shows a continuously declining surface heat flux and a geotherm that changes accordingly.

Density profiles corresponding to the conductively evolving geotherm and computed composition profiles (i.e., degree of depletion and basaltic crust) are computed, and from these the density defect thickness is determined as a function of time (see Figure 4.1). From this we obtain the zero density defect thickness time, which is the time required for the oceanic lithosphere to become neutrally buoyant.

The extrusion temperature, which occurs as a boundary condition in the solution of (4.2) and which is directly linked to the potential temperature (see Figure 4.1), is used as a control parameter, to select for different stages in the thermal evolution of a planet. The gravitational acceleration is implicitly present in the pressure dependent depth of solidus and liquidus, and can thus be used as a control parameter to select for different planets. The computation of the thermal evolution of an oceanic lithospheric column depends

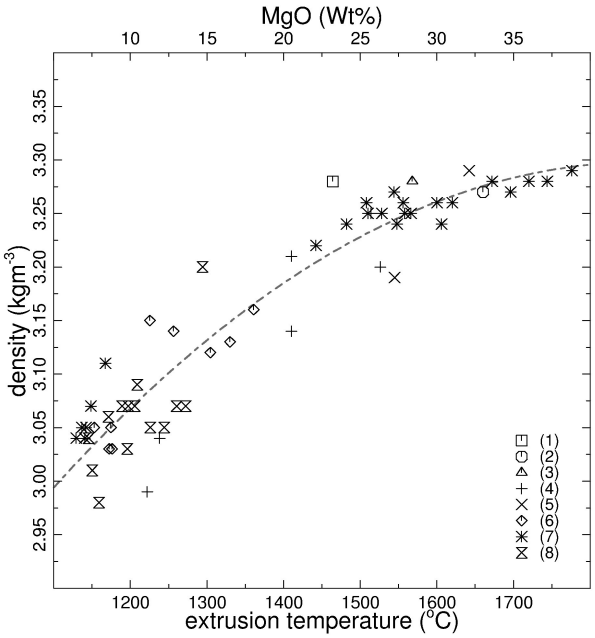

Figure 4.2: Primitive magmatic rock densities as a function of MgO content or extrusion temperature, of 58 basalts, komatiitic basalts, komatiites and a picrite. The quadratic best fit for the entire set (see equation (4.3)) is shown by the dashed curve. References for the data are: (1) Parman et al. (1997), (2) Green et al. (1975), (3) Smith et al. (1980), (4) Ludden and Gelinas (1982), (5) Nishihara and Takahashi (2001), (6) Kerr et al. (1996), (7) Puchtel et al. (1998) and (8) Arndt and Nesbitt (1982).

on the surface temperature, T_{surf}, which is specified. This makes up the third control parameter. The potential mantle temperature, gravitational acceleration and the surface temperature span the parameter space which we will investigate for different lithosphere thicknesses.

4.2.2 Model parameters

Relevant input parameters for the melting and cooling models are listed in Table 4.1.

The surface temperature, T_{surf}, of the planet we are dealing with defines the thermal upper boundary condition of the 1-D cooling model for a mantle column. For the Earth, T_{surf} has been buffered for most of its history by the presence of liquid water on the surface. Oxygen isotope studies suggest the presence of liquid water and possibly even oceans as far back as 4.4 Ga (Wilde et al., 2001; Peck et al., 2001). For Venus we only know the present thermal conditions, which show an average T_{surf} of 467^oC. On Mars

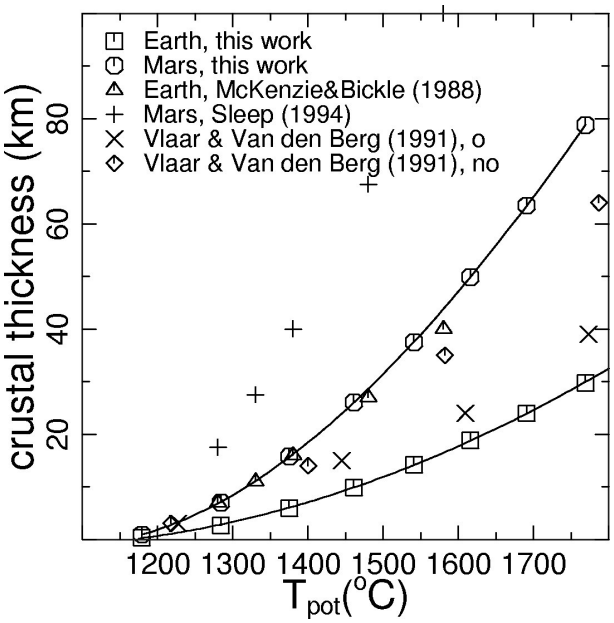

Figure 4.3: Thickness of the crust as produced at mid-ocean ridges, for Earth and Mars. The results of McKenzie and Bickle (1988) do not include the effect of the overburden pressure of the crust, and therefore give an overestimate of the thickness. The results for Mars by Sleep are those of McKenzie and Bickle (1988) divided by a factor of 0.4 to correct for different gravity and a somewhat more iron-rich composition of the basalts (Sleep, 1994). The results of Vlaar and Van den Berg (1991), with (o) and without (no) including the effect of the crustal overburden, clearly show that the crustal overburden is an important effect that should not be neglected.

the average T_{surf} is significantly lower, $\sim -55^oC$. However, morphological features strongly reminiscent of flow channels suggest that liquid water may have been present on the surface in the early history of the planet (e.g. Jakosky and Phillips, 2001), which implies that more present day Earth-like surface conditions may have prevailed during the planet's earlier evolution (Baker, 2001). Based on this information, we find neutral buoyancy ages as a function of potential temperature and gravitational acceleration for two different values of T_{surf}. The first is 0^oC, which is representative of Earth and perhaps Mars during most of its history. The second value applied is 467^oC, which is representative of present time Venus, and possibly for an unknown part of its history.

We also consider the effect of varying T_{surf} for a fixed value for the gravitational acceleration ($9.8ms^{-2}$) for a range of potential temperatures.

We do the experiments using a number of values for the lithosphere thickness, spanning the range of values expected for the terrestrial planets during their evolution.

The present oceanic lithosphere thickness on Earth is estimated to be about 100-125 km (Parsons and Sclater, 1977; Stein and Stein, 1992). Convection scaling analysis (e.g. Parsons and McKenzie, 1978) indicates that this value will be smaller for higher mantle temperatures. Additionally, the strong temperature dependence of viscosity (e.g. Karato and Wu, 1993) will also decrease the lithosphere thickness for higher mantle temperatures.

For Venus and Mars, the lithosphere thickness is not well constrained for the present stagnant lid situations, and are more uncertain for hypothetical plate tectonics scenarios. Smrekar and Parmentier (1996) constructed numerical convection models for the interaction of mantle plumes with boundary layers applied to Venus and found that models with a lithosphere of 100-150 km thickness resulted in the best fit with data for large volcanic rises on Venus. Independently, Nimmo and McKenzie (1996) found that a conductive lid of less than 150 km thickness results in the best fit of their gravity models to observations. These results indicate that the present lithospheric thickness of Venus is probably less than 150 km, and may be relatively close to that of the Earth. However, we need to stress that these are lithosphere thickness values for the present stagnant-lid situation. In a plate tectonics setting, the thickness may be different but is probably less because of the more efficient transport of heat to shallow levels in a plate tectonics setting relative to a stagnant lid regime.

Spherical convective numerical models of the thermal evolution of Mars by McKenzie et al. (2002) show lithosphere thicknesses of around 200 km for the present and less than 100 km for the early history of the planet, again in a stagnant lid regime. Earlier work by Solomon and Head (1990), based on estimates of the elastic thickness of the Martian lithosphere, resulted in mechanical lithosphere thicknesses of less than 20 up to 140 km. They used the conversion chart of McNutt (1984), which defines the mechanical lithosphere thickness as the depth of the 600^oC isotherm. Extrapolation to mantle temperatures results in estimates for the thermal lithosphere that are approximately twice these values.

These constraints allow us to pick the lithosphere thickness for the different models. We use a thickness of 100 km for a model with surface temperature 0^oC, representing the Earth and Mars. For Mars, we also run a model with a 200 km lithosphere. For Venus, with a surface temperature of 467^oC, we use a lithosphere thickness of 150 km. Obviously, smaller thickness values are required for the earlier, hotter histories. We will investigate the sensitivity to lithosphere thickness to determine the magnitude this effect.

4.3 Results

First we illustrate the development of the density defect thickness $d.d.t.$ as a function of time for the model Earth and Mars in Figure 4.4. In each case the lithospheric column has a positive $d.d.t.$ at t=0 (the time of formation), which means that it is positively buoyant. For the present-day Earth ($T_{pot} = 1353^oC$ in Figure 4.4a) we see that the column becomes negatively buoyant (crosses the $d.d.t. = 0$ line) after about 25 Myr, which is close to earlier results (30 Myr) of Vlaar and Van den Berg (1991). At lower potential temperatures, negative buoyancy is reached in a shorter time. Higher potential

temperatures result in greater neutral buoyancy ages, and we observe in this figure that the $d.d.t.$-curve corresponding to a potential temperature of 1625^oC shows a constant positive buoyancy that is no longer decreasing with age after about 150 Myr. In Figure 4.4b, model Mars shows similar curves, which, as a result of the lower gravitational acceleration, have been shifted upwards by about 1 km on the $d.d.t.$ axis. As a consequence, longer neutral buoyancy ages are observed for low mantle temperatures, and neutral buoyancy is no longer reached for potential temperatures representative of Earth.

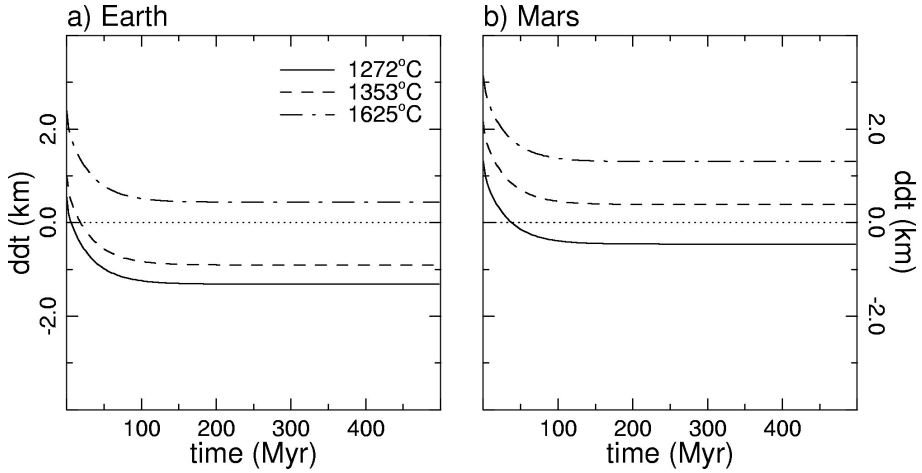

Figure 4.4: Density defect thickness time series for the Earth (a) and Mars (b) for potential mantle temperatures of 1272^oC (solid curves), 1353^oC (dashed curves) and 1625^oC (dash-dotted curves). For positive values of the d.d.t. the oceanic lithosphere is buoyant.

Resulting neutral buoyancy times (density defect thickness $d.d.t. = 0$) as a function of potential temperature and gravitational acceleration are presented in Figure 4.5a for $T_{surf} = 0^oC$ and a lithosphere thickness of 100 km. The horizontal axis represents the potential mantle temperature, and the vertical axis shows the gravitational acceleration, which enables the comparison of the different terrestrial planets. The contours are lines of equal neutral buoyancy times. Note that the solidus temperature at the surface is 1125^oC, which implies that no differentiation takes place below this temperature. This means that compositional buoyancy due to compositional differentiation is lost and that any negative deviation from the adiabat results in a negative buoyancy. As a consequence 'lithosphere' in a mid-ocean ridge setting would immediately become negatively buoyant due to cooling. The planet specific gravitational accelerations are indicated in the figure as horizontal lines and labeled for Earth, Venus, and Mars. The maximum contour that is included is that of 500 Myr. Here the neutral buoyancy age is increasing asymptotically to infinity for increasing potential temperature, indicating that for higher values of the potential temperature the lithosphere does not become negatively buoyant at all. The dash-dotted

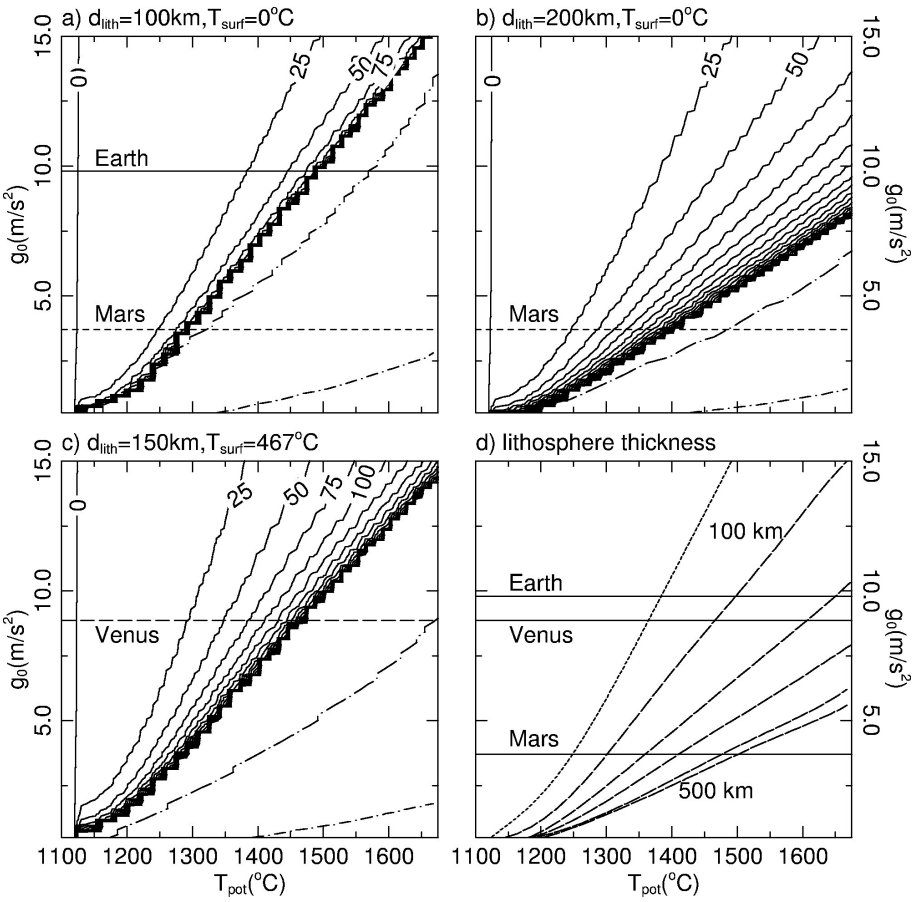

Figure 4.5: Frames a-c show contours of the neutral buoyancy (density defect thickness = 0) times. a) Surface temperature is 0^oC and lithosphere thickness is 100 km, potentially applicable to both Earth and Mars. The gravitational accelerations for these terrestrial planets are included as horizontal lines (solid: Earth, dashed: Mars). b) Surface temperature is 0^oC and lithosphere thickness is 200 km, potentially applicable to Mars, including the gravitational acceleration of Mars (dashed line). c) Surface temperature is 467^oC and lithosphere thickness is 150 km, potentially applicable to Venus, including the gravitational acceleration of Venus (long-dashed line). d) Variation of neutral buoyancy times as a function of lithosphere thickness for a surface temperature of 0^oC. Gravitational acceleration values for Earth, Venus and Mars are indicated by solid lines. The 25 Myr isoline is indicated by the dotted curve. Dashed curves indicate the position of the 500 Myr isoline for lithosphere thicknesses of 100 km, 150 km, 200 km, 300 km and 500 km.

curves in Figure 4.5a indicate where the fixed lithospheric thickness, of in this case 100 km, is equal to the thickness of the compositional stratification (basaltic crust and harzburgitic root) produced at mid-ocean ridges (long dashes) and where the lithospheric thickness is equal to the crustal thickness (short dashes). Lithospheric thickness is greater to the left of these curves. Results to the right of the latter curve are ignored since the expected internal convection in the crust is not included in the current model. For the present-day Earth, with a potential temperature of $1300 - 1350^oC$, we obtain a neutral buoyancy age for oceanic lithosphere of about 20-25 million years, which is consistent with earlier estimates of 40-50 Myr (Oxburgh and Parmentier, 1977), 30 Myr (Vlaar and Van den Berg, 1991), and 20 Myr (Davies, 1992). For a hotter Earth the neutral buoyancy age increases to about 100 million years near $T_{pot} \sim 1500^oC$ and much longer times are obtained for only slightly higher temperatures. For Mars (dashed line), neutral buoyancy times already rise to hundreds of million years for a moderate potential temperature below 1300^oC, in line with much stronger compositional differentiation under low-gravity conditions on Mars (Schott et al., 2001). The Martian lithosphere may however be thicker than 100 km. When assuming a thicker lithosphere of 200 km for Mars, as shown in Figure 4.5b, neutral buoyancy ages are less than 150 Myr below potential temperatures of 1350^oC, and rise to 500 Myr around 1400^oC.

When applying a surface temperature of 467^oC, consistent with present-day Venus, cooling of the lithosphere becomes slower and therefore neutral buoyancy ages become longer (Figure 4.5c, where a lithosphere thickness of 150 km is applied). For a Venusian gravitational acceleration neutral buoyancy ages of about 500 million years can be observed for a potential temperature of 1480^oC.

The effect of lithosphere thickness on the neutral buoyancy age is illustrated in Figure 4.5d for a surface temperature of 0^oC. Solid lines indicate the position of the terrestrial planets. The dotted curve indicates the 25 Myr isoline of the neutral buoyancy age. The position of this curve is relatively insensitive to lithosphere thicknesses, since initial cooling of the oceanic lithosphere takes place at shallow levels. The dashed curves indicate 500 Myr isolines of the neutral buoyancy age for lithosphere thicknesses of 100 km, 150 km, 200 km, 300 km and 500 km. It is evident that a greater lithosphere thickness allows cooling of the lithosphere to deeper levels and lower temperatures, decreasing its buoyancy. Thus a thick lithosphere may significantly prolong neutral buoyancy ages.

The effect of surface temperature on the neutral buoyancy age is more clearly illustrated in Figure 4.6. In this figure, the neutral buoyancy age is contoured as a function of potential temperature on the horizontal axis and T_{surf} on the vertical axis for a constant Earth-like gravity of 9.8 ms^{-2} and a lithosphere thickness of 150 km. It is evident that the effect of T_{surf} is greatest for high mantle potential temperatures near the asymptotic increase of the neutral buoyancy age. For the present-day Earth's potential temperature of about 1350^oC, an increase in T_{surf} of about 500^oC is required to double the neutral buoyancy age from 20 to 40 Myr. In general, the higher T_{surf} of Venus causes a shift in the neutral buoyancy age contours of up to 125^oC along the the potential temperature axis. It is clear from this figure that the difference in surface temperature between Earth and Mars is not an important factor in explaining the different types of dynamics.

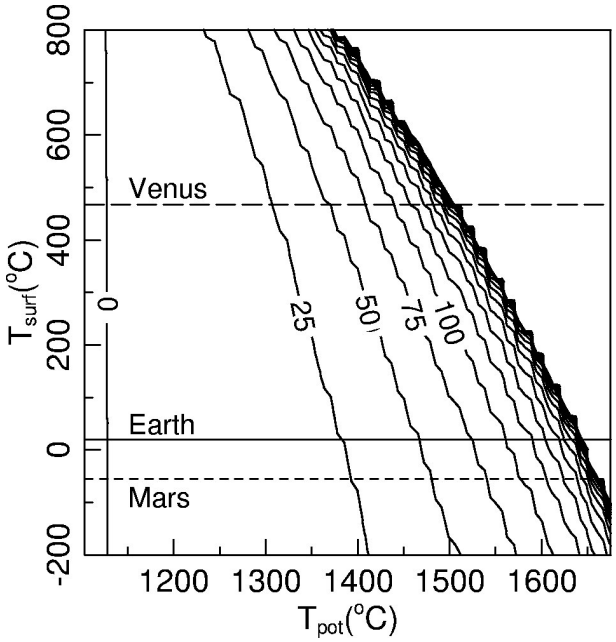

Figure 4.6: Neutral buoyancy (density defect thickness = 0) times for a constant gravitational acceleration of 9.8 ms^{-2} and lithosphere thickness of 150 km as a function of potential temperature and surface temperature. The horizontal lines indicate the position of Venus (long-dashed), Earth (solid) and Mars (dashed).

4.4 Discussion

4.4.1 Plate tectonics on Earth

The accretion of the Earth, the differentiation of the core (Horedt, 1980), and the decay of short-lived isotopes (Ruff and Anderson, 1980) each supplied enough heat to melt at least a significant part of the Earth. Furthermore, geochemical evidence (Murthy, 1992a) and modeling efforts (e.g. Abe, 1993a,b, 1997) indicate that the early Earth had a magma ocean for some time. This means that the potential temperature of the mantle has dropped from a very high value outside the scale of the horizontal axis of Figure 4.5a to a present-day value of about $1300 - 1350^oC$, and that the Earth passed through stages covered by most of the Earth ($g_0 = 9.81ms^{-2}$) line in Figure 4.5a. We do not know, however, the exact timing of the cooling. The high magnesium contents of Archean komatiites indicate extrusion temperatures of $1520-1580^oC$, corresponding to potential temperature of $1600 - 1900^oC$ (Nisbet et al., 1993). This is based on the assumption of dry melting, which was validated by Arndt et al. (1998). Others, however, propose that the generation of komatiites took place under hydrous conditions at mantle temperatures only 100^oC

higher than the present (e.g. Stone et al., 1997; Parman et al., 1997), suggesting potential mantle temperatures during the Archean that are only moderately higher than present-day.

The difficulty of maintaining plate tectonics at higher mantle temperatures in the Earth has already been addressed by different authors (Sleep and Windley, 1982; Vlaar, 1985; Vlaar and Van den Berg, 1991; Davies, 1992). The opposing effect of a more komatiitic composition of the crust was discussed by Arndt (1983) and Nisbet and Fowler (1983). They suggest that a thin (comparable to the present) oceanic crust rich in komatiites may allow plate tectonics to operate, and that the reduced resistive forces as a consequence of the higher mantle temperature and temperature dependent rheology could make it more efficient. Upwelling in a mid-ocean ridge system in a hotter mantle, however, produces a thick crust, as the supersolidus path of the ascending material is longer. Our results take into account the temperature dependent composition of the basaltic crust and show that this thicker crust, although denser due to its composition being closer to komatiitic, is not dense enough to facilitate subduction at potential temperatures above about 1500^oC for the Earth on reasonable time scales, confirming the results of Vlaar and Van den Berg (1991) which did not include the effect of higher temperatures on melt product composition and density. We note, however, that the buoyancy approach is only one of many to investigate the conditions under which plate tectonics may operate. Other factors include stresses required to initiate subduction (e.g. McKenzie, 1977), bending of the lithosphere (e.g. Conrad and Hager, 2001), and temperature dependent rheology with strong impact on the mechanical coherency of subducting lithosphere (Van Hunen, 2001; Van Hunen et al., 2003), which may be important but are beyond the scope of this paper.

4.4.2 Plate tectonics on Venus

Nimmo and McKenzie (1998) estimate the potential mantle temperature of Venus to be about $1300 - 1500^oC$. Because of the history of Venus (e.g., accretion, core differentiation) and the composition (e.g., radiogenic heating) being similar to Earth, one may expect that Venus has experienced a hot early history as well, perhaps including a magma ocean period. Calculations indicate that the surface heat flux of the planet is about half of the radiogenically produced heat, which means that the planet must be heating up (Nimmo and McKenzie, 1998). From crater count studies, Venus appears to have undergone global resurfacing about 300-600 Myr ago (Schaber et al., 1992; Nimmo and McKenzie, 1998). No evidence of plate tectonics has been found. So if Venus has had plate tectonics, it must have been before the (last?) global resurfacing. Episodic plate tectonics has been suggested for Venus (Turcotte, 1993), and also on the basis of our results there is no reason to disqualify Venus for plate tectonics. Assuming a more or less constant surface temperature during (part of) the history of the planet, Figure 4.5c shows that reasonable neutral buoyancy ages are possible for potential temperatures below about 1450^oC, or even below about 1650^oC when assuming a more Earth-like surface temperature (see Figures 4.5d and 4.6). But although buoyancy considerations allow plate tectonics on present-day Venus, it does not take place. The atmosphere of Venus is dry, and if this can be extended to the mantle, this increases the mantle strength, fault friction and melting temperature relative to the Earth (Nimmo and McKenzie, 1998). Because dry rocks are significantly

stronger than hydrous rocks (Chopra and Paterson, 1984; Karato, 1986), plate tectonics could be hindered by this effect. Indeed, the present-day difference in tectonic style between Earth and Venus has been ascribed to the presence of water in the mantle of the former and the absence in the latter planet (Mackwell et al., 1998). Alternatively, the accumulation of compositionally buoyant mantle material, residue from partial melting, in the shallow upper mantle may have a stabilizing effect on the lithosphere (Parmentier and Hess, 1992).

4.4.3 Plate tectonics on Mars

Although different in scale and intensity, linear patterns of rock magnetization on the southern hemisphere have been linked with magnetic striping found on the Earth's ocean floors, and a similar plate tectonic origin has been suggested (Acuña et al., 1999; Connerney et al., 1999). Sleep (1994) interprets surface features of Mars in a plate tectonic framework. Nimmo and Stevenson (2000) investigate the link between surface heat flow and the planetary magnetic field and suggest that the presence of a Martian magnetic field during the first 500 Myr may have been related to a process causing a high surface heat flux such as plate tectonics. Spohn et al. (2001) show cooling histories for Mars based on parameterized models for different modes of heat transfer, including a similar scenario with early plate tectonics followed by a stagnant lid regime. However, the rapid formation of a thick (several hundred kilometer) gravitationally stable and geochemically depleted layer in the Martian mantle in models of Schott et al. (2001) would argue against an early plate tectonic history for Mars. So far, no robust evidence for plate tectonics on Mars has been found, and Mars presently appears to be in the stagnant lid regime (Reese et al., 1998). Our results show that buoyancy considerations allow plate tectonics only for a relatively small range of potential temperatures, below approximately $1300-1400^oC$ (Figure 4.5a,b). Since Mars has a higher surface to volume ratio than Earth, one would expect the planet to cool faster. However, the opposing effect of the early formation of a several hundred kilometer thick buoyant layer of melt residue will strongly reduce the efficiency of convective cooling of the planet (Schott et al., 2002). As a consequence, Mars possibly never cooled down sufficiently to reach the operational temperature window for Earth-like plate tectonics, and might well have a potential temperature above $1300 - 1400^oC$. The presence of such a thick depleted root might have obstructed large-scale melt extraction from the mantle required for massive volcanism which was absent during the past 1-2 Gyr of Mars' history, despite the possibly elevated internal temperature. Recently, indications of less widespread recent volcanism (< 100 Myr) have been found (Hartmann et al., 1999), providing arguments for an elevated internal temperature.

4.5 Conclusions

Based on buoyancy arguments, we find the following maximum potential mantle temperatures for which neutral buoyancy is reached on reasonable time scales (within 500 Myr): 1500^oC for Earth, 1450^oC for Venus (or 1650^oC when assuming cooler surface condi-

tions in the earlier history of the planet), and $1300 - 1400^oC$ for Mars. Whether plate tectonics will actually take place also depends on other factors, like water content of the mantle, however. Geological evidence indicates that plate tectonics has been active on Earth since the Proterozoic (Hamilton, 1998), and possibly much earlier (De Wit, 1998). The potential temperature at which oceanic lithosphere may become negatively buoyant within 500 Myr, 1500^oC, might be representative of the late Archean, a time which also appears to mark a change in the geology (Richter, 1988). We speculate that at this time the geodynamic regime changed from a different mechanism to modern style plate tectonics dominated by dipping slabs sinking into the mantle. On the basis of buoyancy arguments, we propose that it is possible that Venus had a period of plate tectonics during its history, although this may have been hindered by a high planetary surface temperature. It appears unlikely that Mars had plate tectonics during its early, presumably hotter, history, because of its relatively low operational temperature window below $1300 - 1400^oC$ above which negative buoyancy is not reached on reasonable time scales.